LAWRENCE
LIVERMORE
NATIONAL
LABORATORY

LLNL-JRNL-609319

New Materials for Methane mitigation from dilute and medium-concentration sources

J. Kim, A. Maiti, L. Lin, J. K. Stolaroff, B. Smit, R. D. Aines

January 3, 2013

Nature Communications

Disclaimer

New Materials for Methane mitigation from dilute and medium-concentration sources

Jihan Kim[1], Amitesh Maiti[2,*], Li-Chiang Lin[3], Joshuah K. Stolaroff[2], Berend Smit[1,3,4] and Roger D. Aines[2]

[1]Materials Sciences Division, Lawrence Berkeley Laboratory, Berkeley, CA 94720
[2]Physical and Life Sciences Division, Lawrence Livermore National Laboratory, Livermore, CA 94550
[3]Department of Chemical and Biomolecular Engineering, University of California, Berkeley, CA 94720
[4]Department of Chemistry, University of California, Berkeley, CA 94720

Methane (CH_4) is a dangerous greenhouse gas, second only to CO_2, and is emitted into the atmosphere from a variety of sources at different levels of concentration. However, unlike CO_2, which has a quadrupole moment and can be captured both physically and chemically in a variety of solvents and microporous solids, methane is completely non-polar and interacts very weakly with most materials systems. Thus, methane mitigation through capture and utilization poses a significant technological and chemistry challenge that can only be addressed through extensive materials screening and ingenious molecular-level designs. In this work we report systematic *in silico* studies on the effectiveness of two different classes of capture materials, i.e., liquid solvents (including Ionic Liquids) and nanoporous zeolites. While none of the common solvents and ionic liquids appears to possess enough affinity toward methane to be of practical use, systematic screening of over 87000 zeolite structures led to the discovery of a few candidates that have reasonable methane sorption capacity as well as appropriate CH_4/CO_2 and/or CH_4/N_2 selectivity to be technologically promising. We use free-energy profiling and geometry analysis in these candidate zeolites to understand and analyze how the distribution and connectivity of pore structures and binding sites can lead to enhanced sorption of methane while being competitive with CO_2 sorption at the same time.

Methane is a substantial driver of global climate change, contributing 30% of current net climate forcing [1]. Additionally, concern over methane is mounting due to leaks associated with rapidly expanding unconventional oil and gas extraction and the potential for large-scale release of methane from the Arctic [2]. At the same time,

* E-mail: amaiti@llnl.gov

methane is a growing source of energy [3] and aggressive methane mitigation is increasingly recognized as a key to avoiding dangerous levels of global warming [4, 5].

Methane is emitted at a wide range of concentrations from a variety of sources, including natural gas systems, enteric fermentation (livestock), landfills, coal mining, manure management, wastewater treatment, rice cultivation, and a few combustion processes. We can generally group the methane concentrations of sources into three categories: high purity (> 90%), medium purity (5-75%), and dilute (< 5%). High-purity methane can be sold to the commodity natural gas market or converted to other chemicals (e.g. methanol, carbon black) by current industrial practices. Medium purity methane includes landfill gas, coalmine drainage gas, anaerobic digester gas, and low-quality gas from fossil formations. A variety of technologies have been developed for generating electricity or high-grade process heat from medium-purity methane, including technologies, such as the homogeneous charge gas engine that operate just above the methane flammability limit in air (5%). Small or inconvenient flows of medium purity methane are often simply flared [2]. Treatable dilute methane sources are some of the largest in total emissions, including coal mine ventilation air, manure storage headspace, and animal feeding house ventilation air. Some technologies have been developed for oxidizing dilute methane, such as the thermal flow-reversal reactor, but they generally yield only low-grade heat or small amounts of electricity as a co-benefit.

It is highly desirable to be able to concentrate a dilute methane stream to medium purity in order to effectively utilize the energy, or to concentrate a medium purity stream to a high purity stream in order to convert it to a liquid or sell it. Conversion is especially attractive for many small or remote sources. Purification of some medium and higher purity natural gases is currently practiced industrially by sorption of the non-methane components (CO_2, H_2S). The practice becomes uneconomic or impractical below about 40% methane [6]. For methane concentrations below 40%, or for separation of methane from air rather than acid gases, we would like a sorbent for methane itself.

In this contribution, we explore the possibility of a sorbent for methane purification. We consider the general problems of (1) concentrating a medium purity stream to the high-purity range and (2) concentrating a dilute stream to the medium purity range. For purposes of analysis, our proxies for these cases are (1) a low-quality natural gas (simplified as 30% methane and 70% CO_2 by mole fraction at a total pressure of 70 bar), and (2) coal mine ventilation air (simplified as 1% methane, 1% CO_2, and 98% N_2 at a total pressure of 1 bar). Both of these are potential large scale, high-impact applications for a sorbent for methane. The example cases illustrate two general

characteristics of methane purification. First, because processes related to the ones that produce methane also produce CO_2, almost all natural methane streams contain significant levels of CO_2. Second, for dilute streams, N_2 is the dominant component to exclude. O_2 is also abundant, but for combustion applications, it is desirable to carry at least as much O_2 as CH_4 through the process.

For going from medium to high purity methane a sorbent selectivity of CH_4 over CO_2 greater than 1 is required and, generally, the higher the selectivity, the fewer absorption-desorption cycles required to reach desired purity. For going from dilute to medium purity, the selectivity of CH_4 over N_2 is more important for determining the number of cycles. At the same time, CH_4/CO_2 selectivity not much less than 1 remains a requirement, for otherwise the presence of CO_2 can potentially reduce the CH_4 uptake and degrade its flaring efficiency.

Liquid Solvents for methane capture: One would expect liquids to be poor absorbers of methane, given its highly symmetric structure, zero dipole and quadrupole moments, low polarizability, and low chemical reactivity. Perhaps this explains why the scientific literature reports only a handful of measurements of methane solubility in just a few solvents. We still deemed it important to explore the liquid space for several reasons: (1) a good liquid solvent for methane could not only be used as a capture agent, but such a solvent could be injected to break down methane hydrate (clathrate), and extract methane from this potentially huge untapped energy source [7, 8, 9]; and (2) there have been recent experimental attempts of exploring novel solvents (Ionic Liquids) for efficient absorption [10] and catalytic conversion [11] of methane; a systematic *in silico* study could contribute greatly to such progress.

In order to compute methane solubility in liquids we adopted an implicit solvent method, i.e., COSMO-RS [12, 13], in which one represents both the solute and solvent molecules by the histogram of their surface screening charges called the σ-profile. All interactions, including coulombic, van der Waals, and hydrogen bond interactions are then defined in terms of these σ-profiles. One can use this formalism to compute the partition function, the Gibbs free energy, and many other thermodynamic quantities, including pseudo-chemical potentials (μ*) [14], which are used to compute the solubility of a solute in a solvent through the following formula:

$$x_{solute} = \exp\{-(\mu^*_{solvent} - \mu^*_{self})/k_B T\}, \qquad (1)$$

where x_{solute} is the molar solubility of the solute in the solvent, $\mu^*_{solvent}$ and μ^*_{self} are respectively the pseudo-chemical potentials of the solute in the solvent environment and in its own liquid environment, and k_B and T are the

Boltzmann constant and the absolute temperature. When the solute is dissolving from the gas phase, one needs to relate the quantity μ^*_{self} to the chemical potential in the gas phase, which can be expressed as a function of the gas fugacity [15]. However, since our liquid exploration involved a fixed pressure (1 bar) and a fixed temperature (298 K) we found it more convenient to use μ^*_{self} as a fitting parameter so as to match the experimental solubility of all relevant gases, i.e., CH_4 [9, 16], N_2 [17, 18], and CO_2 [19] in one standard solvent, i.e., ethanol.

As in our previous work [20], the surface screening charges (and the corresponding σ-profiles) were computed using the Density Functional Theory (DFT) code Turbomole [21], the Becke-Perdew (BP) exchange-correlation functional [22, 23], and an all-electron representation using the triple-zeta valence basis set with polarization (TZVP) [24, 25]. From extensive tests on the aqueous solubility of a large dataset of drug molecules or organic solutes it appears that COSMO-RS incurs an average error of the order of 0.3-0.5 log units [26]. Based on the above, an accuracy of the computed solubility to within a factor of 2-3 can be considered reasonable.

First we wanted to explore the feasibility of liquid solvents to concentrate coal-mine ventilation air, represented by (in mole fraction) 1% CH_4, 1% CO_2, 98% N_2 at a total pressure of 1 bar. The aim was to create an output stream with > 5% CH_4. The presence of O_2 was not considered explicitly just for simplicity, and it was assumed that the output stream will have sufficient O_2 to be able to flare the methane. One major requirement for this technology to work is that the amount of CO_2 in the output should not be too high, for that would competitively inhibit the reaction of methane with O_2 making the flaring process inefficient. The above requirements can be translated into the following target selectivities: $CH_4/N_2 > 5$ and $CH_4/CO_2 \sim 1$ (the higher the better). With the above in mind, we computed the solubilities (using eq. (1)) of CH_4, N_2, and CO_2 in 73 common room-temperature liquid solvents at T = 25 ^oC and P = 1 bar. A wide variety of representative solvents were chosen, including alkanes, cyclo-alkanes, alkenes, alkynes, aromatics, alcohols, aldehydes, ether, ketones, amines, and thiols.

Fig. 1 plots the ratio of CH_4 and N_2 solubility (expressed as CH_4/N_2 selectivity) on the y-axis and the corresponding CH_4 solubility (expressed as the Henry's constant in mol/kg/bar) on the x-axis. Interestingly there are many solvents with CH_4/N_2 selectivity > 5, with 1-octanamine and 1-octanethiol having values > 10. The solvents with the highest CH_4 solubility appear to be the small alkanes like pentane, cyclo-pentane, hexane, etc., as well as carbon-disulfide (CS_2). All of these solvents also have desirable CH_4/N_2 selectivity values of ~ 8. Unfortunately, the

Henry's constant is too low, being ~ 0.044 mol/kg/bar even for the best solvent, i.e., pentane. For an inlet partial methane pressure of 0.01 bar, this would amount to a loading of only $4.4x10^{-4}$ mol/kg, which does not make it economically viable. Additionally, Fig. 2 shows that even for the alkanes the highest value of the CH_4/CO_2 selectivity is low, being only 0.36 for cyclo-decane and 0.34 for pentane. This means that in the output stream there will be roughly three times more CO_2 as compared to CH_4, which will make flaring inefficient.

Given the recent interest in Ionic Liquids (ILs) [27], we have also used the above procedure to screen a few classes of ILs, with cationic classes including imidazolium, ammonium, phosphonium, and pyridinium, and anions including BF_4, PF_6, and TF_2N [15, 27]. Consistent with limited available experimental data [10, 28], we find that the highest CH_4 solubility in these classes of ILs occurs in the [ammonium][TF_2N] systems with a Henry's constant of less than 0.01 mol/kg/bar, i.e., four times less than that in pentane. Not surprisingly, given an ionic environment, the CH_4/CO_2 selectivity in ILs is also much worse than regular alkanes, being typically less than 0.1.

The above analysis clearly demonstrates that liquid solvents, including ionic liquids, are not suitable for concentrating and utilizing methane from low to medium emission sources – the methane solubility is too low, and the CH_4/CO_2 selectivity is not favorable. Thus, we turned to another system with a large number of possible structural and compositional varieties, i.e., nanoporous materials, like zeolites.

Zeolites for methane capture: Zeolites are porous materials commonly used as adsorbents. Due to their diverse topology resulting from various networks of the framework atoms, zeolites can be used for many different types of gas separations and storage applications. In this work, we analyzed 190 experimentally realized IZA structures and over 87,000 predicted crystallography open database (PCOD) structures from Deem's hypothetical zeolite database [29] to search for materials suitable for methane mitigation. The Henry's constant and the pure component adsorption isotherms for CO_2, CH_4, N_2 gas molecules were computed using our highly efficient graphics processing units (GPU) code [30, 31] and the ideal adsorption state theory (IAST) then applied to estimate the mixture component uptake to reproduce the aforementioned conditions relevant to methane separations [32]. In our simulations, all interactions were described at the classical force field level with atomic partial charges (for Coulomb interactions) and 12-6 Lennard-Jones parameters (for van der Waals interactions) taken from Garcia-Perez et al. [33] between gas molecules and the zeolite framework . The framework was assumed to be rigid throughout the

simulation, an assumption that is considered to be reasonable in zeolite structures [34].

Due to their non-polar nature, the interaction between the CH_4 molecules and the framework atoms are generally much weaker than that compared to the polar CO_2 molecules. Accordingly, finding zeolite structures that would simultaneously lead to large adsorbed CH_4 concentration (relative to adsorbed CO_2) and high CH_4 loading poses a significant challenge even with the large number of diverse zeolite structures at our disposal. For mixtures that contain methane at relatively low pressure, the binding energy of methane is the primary factor that determines the performance of the structure. On the other hand, for separations that occur at higher pressures, the CH_4-CH_4 interaction could also play a significant role. Thus, we expect that the total pressure of the initial mixture gas will largely dictate the type of materials optimal for methane mitigation.

First, we performed the zeolite screening for the application involving a low-quality natural gas mixture feed consisting of 30% CH_4 and 70% CO_2 (in mole fraction) at 70bar and 300K. Fig. 3 indicates the adsorbed CH_4 concentration (mole fraction) in the adsorbed gas mixture as a function of the adsorbed amount of methane (i.e. methane loading) for all of the IZA and the predicted zeolite structures. The results immediately reveal an IZA structure, SBN, that stands out in its performance -- roughly 2.75 (mol/kg) CH_4 adsorbed and 45% CH_4 adsorbed concentration, corresponding to a CH_4/CO_2 selectivity of ~ 1.9. We also utilized the recently published force field from Sholl and co-workers [35] to compute the CO_2 adsorption isotherms, which predicts even better overall performance (see Fig.3) for SBN with reduced CO_2 uptake for all of the pressure values. To further test the robustness of our finding, sensitivity analysis was conducted by changing (in steps of 1%) the SBN lattice parameters from -3 to +3% of the original optimized value of a = 14.37 Å, b = 12.45 Å, and c = 13.85 Å. For each perturbed structure the lattice constants were kept fixed while the atomic coordinates were optimized using density functional theory (DFT) with the quantum code SIESTA [36]. As shown in Fig.3, all of the perturbed SBN data points are close to the original SBN data, indicating that in spite of a small dependence of its performance on force field parameters and lattice constant SBN is clearly one of the best structures for methane capture.

To further explore the reason behind the exceptional performance of SBN, we plot in Fig. 4 the simulated adsorption isotherm curves and the free energy landscapes in this zeolite for both CO_2 and CH_4. Within the idealized SBN structure, blue (red) represents low (high) energy regions with the rest indicating inaccessible regions. In order to help with the analysis, the adsorption isotherm curves are divided into three regimes based on

the total pressure (i.e. $P < 1$ bar, 1 bar $< P <$ 100 bar, $P >$ 100 bar), representing the Henry regime, strong CH_4-CH_4 interaction regime, and saturation regime, respectively (see Fig. 4). In the Henry regime ($P < 1$ bar), the guest particle-framework interaction dominates the adsorption properties where the Henry's constant K_H = 0.86 mol/kg/bar and 0.52 mol/kg/bar for CO_2 and CH_4 respectively, leading to higher uptake of CO_2 in this region. The difference can be explained by comparing the binding energy values (CH_4: -22.09 kJ/mol and CO_2: -28.57 kJ/mol) of the two molecules. At $P \sim 5$ bar the two isotherm curves intersect each other, beyond which the CH_4 uptake becomes larger. To understand the increased uptake of CH_4 in SBN at $P > 5$ bar we analyze in Fig. 4 the free energy profiles of CO_2 and CH_4. We find that the CH_4 adsorption sites are highly localized with each site connected to three nearest neighbor adsorption sites (indicated by yellow arrows in Fig.4) with a separation barrier. The distances between these adsorption sites range from 4 to 4.6 Å with the average at around 4.33 Å. Such separation values align closely with the minimum energy distance of two center-of-mass CH_4 molecules, ~ 4.2 Å. On the other hand, the adsorption sites for CO_2 are less distinct from one another, and do not in general correspond to optimal CO_2-CO_2 distances. Interestingly, the CH_4 isotherm in SBN is higher than the CO_2 isotherm for P up to a few thousand bars, well above the pressures considered for low quality natural gas separations. At pressures of 100 bar or more, the CH_4 loading saturates to 16 molecules/unit cell, equal to the number of distinct CH_4 adsorption sites that can be counted from the free energy profile in Fig.4.

For the coal mine ventilation air comprised of 1% CH_4, 1% CO_2, and 98% N_2 at a total pressure of 1 bar, similar analysis was conducted to evaluate structures suitable for this separation. The three-component IAST was utilized to obtain the mixture loading values from the pure component isotherms. Figure 5(a) shows the results for the IZA and the predicted database zeolite structures. At this condition, the uptake values of these three gases tend to lie within the linear region in the pure component isotherms for most zeolite structures and accordingly, a strong correlation exists between Henry's constant and uptake values at this pressure. Thus, it is not surprising that in our analysis, we found that the top twenty structures (where the metric was taken to be simply the product of the solubility and selectivity) in the predicted zeolite database all possess a CH_4 Henry's constant above 1.36 mol/kg/bar at 300K, which puts them within the top 0.1% of the largest K_H in the database. Zeolite SBN, which has a relatively smaller K_H = 0.52 mol/kg/bar, is predicted to have poor performance for this separation. The analysis of the free energy landscape reveals that most of the top structures are comprised of one-dimensional channels for the CH_4 molecules. In addition, geometry analysis utilizing Zeo++ [37] indicates that the maximum included sphere along

these free paths is of diameter ~ 5-6 Å. Thus, these channels can be characterized as narrow and not cage-like. In general, the zeolite structures with narrow channels can form strong CH_4 binding sites as the number of oxygen framework atoms located within close (~ 3-4 Å) vicinity to the center of the binding sites can be maximized within this topology. On the other hand, cage-like environment tends to provide less number of framework O-atoms at optimum distances from the CH_4, thereby leading to low Henry's constant values.

In this separation, we further focused on zeolite structures that also possess high CH_4/CO_2 selectivity. Fig. 5(b) plots the CH_4/CO_2 selectivity of all structures of Fig. 5(a) as a function of adsorbed CH_4 amount, with open symbols indicating the structures with adsorbed CH_4 molar ratio > 0.08 in Fig. 5(a). The IZA structures with the largest CH_4/CO_2 adsorbed ratio were identified to be ZON and FER, with CH_4 K_H = 1.29 and 1.12 mol/kg/bar respectively. Moreover, we have identified many PCOD structures that has a very large CH_4/CO_2 adsorbed ratio (above 2.00), which can be promising for the separation (e.g. PCOD8301873, PCOD8307399). Although IZA structures such as UFI have even larger CH_4 K_H = 1.39 mol/kg/bar than what is computed for ZON and FER, the CH_4/CO_2 K_H selectivity is only 0.44, much smaller as compared to 0.85 and 0.94 corresponding to ZON and FER, respectively. Analysis of these three structures based on the energy profiles reveal that the number of low energy adsorption sites for CO_2 is larger compared to CH_4, which might partially be responsible for the relatively low CH_4/CO_2 K_H selectivity value in UFI. In general, it is difficult to find common characteristics amongst zeolite structures that possess both large CH_4 K_H and large CH_4/CO_2 K_H selectivity as intricate yet subtle difference in the framework composition seem to make large contributions.

Besides pure silica zeolite structures, we have also conducted large-scale screening on aluminosilicate zeolite structures in which some of the silicon atom are substituted with aluminum atoms with the addition of cations to ensure charge neutrality. Similar work has been conducted in the past to analyze CO_2 adsorption in aluminosilicate zeolite structures [38]. In our analysis, we found aluminosilicate zeolite structures to be in general, sub-optimal for methane reduction as the presence of cations creates strong binding sites for the CO_2 molecule, and subsequently leads to inferior CH_4/CO_2 selectivity values. However, more in-depth study needs to be conducted in order to determine whether we can completely rule out aluminosilicate zeolites as a viable class of materials for methane mitigation. One can also attempt to screen a large database of porous materials such as metal-organic frameworks or ZIFs to identify structures optimal for methane mitigation. Unfortunately, many of the synthesized structures

possess strong interactions between the metal atoms and the CO_2 molecules, and thus are more promising for CO_2 capture. Finally, there have been recent attempts in the literature to utilize activated carbon [39] and graphene [40] for methane capture. Activated carbon could be a great storage medium for relative pure methane [39], but probably not an ideal system to preferentially adsorb CH_4 over CO_2. Graphene, with proper doping and inter-layer spacing could potentially isolate CH_4 [40], but more work needs to be done to optimize such a system for selective methane capture with high loading capacity. Perhaps a large-scale screening approach such as ours could be appropriate for such an exploration.

In summary, with the aim of discovering materials capable of isolating or concentrating methane at minimum energy costs, we have carried out extensive *in silico* screening of a large number of conventional and ionic liquids as well as over 87000 zeolite structures. Cutting-edge computational tools were employed, including a density-functional-theory (DFT)-based quantum-chemical implicit solvent formalism [13] for the liquid solvents and a recently developed highly efficient sorption code [30, 31] for the zeolites that employed classical force fields with well-validated parameter sets. Two specific application areas were targeted, i.e., concentrating methane from a medium concentration source to a high concentration (e.g., purifying a low-quality natural gas) and concentrating very dilute methane stream into one of moderate concentration (e.g., enabling efficient flaring of coal-mine ventilation air). Materials design for both these applications is challenging because both warrant materials that have affinity to methane that is comparable to or even exceeds that to CO_2. In this regard, all the liquids in our investigation fall short – the best overall liquid, pentane, has the required CH_4/N_2 selectivity (~ 8), but low Henry's constant (0.044 mol/kg/bar) and low CH_4/N_2 selectivity (0.33). However, some of the zeolites show considerable promise both in terms of CH_4 uptake capacity and CH_4/CO_2 selectivity. Particularly noteworthy is the zeolite SBN, which has a large number of binding sites that are formed in such a way that maximizes the CH_4-CH_4 interactions, resulting in extraordinarily high performance for concentrating methane from a medium concentration source to a high concentration. For dilute methane, on the other hand, there are zeolites like ZON and FER that possess large K_H CH_4 as well as high CH_4/CO_2 selectivity, making them excellent candidates for concentrating dilute methane stream into moderate concentration. For the latter separation, we have also identified other structures in the predicted zeolite database that could potentially outperform ZON and FER. All these structures comprise of narrow one-dimensional channels that create strong binding sites for CH_4 by having a significant number of framework O-atoms at optimal distances from the CH_4 center.

References

1. Barker, T. *et al.*, (eds). *Climate Change 2007: Mitigation. Contribution of Working Group III to the Fourth Assessment Report of the Intergovernmental Panel on Climate Change*. Cambridge University Press, UK (2007).

2. Stolaroff, J. K., Bhattacharyya, S., Smith, C. A., Bourcier, W. L., Cameron-Smith, P. J. & Aines, R. D. Review of Methane Mitigation Technologies with Application to Rapid Release of Methane from the Arctic. *Environmental Science & Technology* **46**, 6455-6469 (2012).

3. Annual Energy Outlook 2011. *U.S. Energy Information Administration.* Washington, DC (2011).

4. Shindell, D. *et al*. Simultaneously Mitigating Near-Term Climate Change and Improving Human Health and Food Security. *Science* **335**, 183-189 (2012).

5. Near-term Climate Protection and Clean Air Benefits: Actions for Controlling Short-Lived Climate Forcers. *United Nations Environment Programme (UNEP)*.

6. Su, S., Beath, A., Guo, H. & Mallett, C. An assessment of mine methane mitigation and utilisation technologies. *Progress In Energy and Combustion Science, Pergamon-elsevier Science Ltd, 31*, 123-170 (2005).

7. Folger, P. *Gas Hydrates: Resource and Hazard*, CRS Report RS22990 (2010).

8. Luo, Y. T., Zhu, J. H., Fan, S. S. & Chen, G. J., *Chem. Eng. Sci.* **62**, 1000-1009 (2007).

9. Ukai, T., Kodama, D., Miyazaki, J. & Kato, M. *J. Chem. Eng. Data* **47**, 1320 (2002).

10. Kou, Y., Xiong, W., Tao, G., Liu, H. & Wang, T. *J. Nat. Gas Chem.* **15**, 282 (2006).

11. Yu, M., Zhai, L. Y., Zhou, Q., Li, C. P. & Zhang, X. L. *Appl. Catal. A* **419**, 53-57 (2012).

12. Klamt, A. *J. Phys. Chem.* **99**, 2224 (1995).

13. Klamt, A. *COSMO-RS: From Quantum Chemistry to Fluid Phase Thermodynamics and Drug Design*. Elsevier (2005).

14. Ben-Naim, A., *Solvation Thermodynamics*, 1st Ed., Plenum Press, New York, USA (1987).

15. Maiti, A. *ChemSusChem* **2**, 628 (2009).

16. Brunner, E. & Hultenschmidt, W. *J. Chem. Thermodyn.* **22**, 73 (1990).

17. Katayama, T. & Nitta, T. *J. Chem. Eng. Data* **21**, 194 (1976).

18. Kretschmer, C. B., Nowakowska, J. & Wiebe, R. *Industrial and Engineering Chemistry* **38**, 506 (1946).

19. Dalmolin, I. et al. *Fluid Phase Equilibria* **245**, 193 (2006).

20. Maiti, A., Kumar, A. & Rogers, R. D. *Phys. Chem. Chem. Phys.* **14**, 5139 (2012).

21. Schäfer, A., Klamt, A., Sattel, D., Lohrenz, J. C. W. & Eckert, F. *Phys. Chem. Chem. Phys.* **2**, 2187 (2000).

22. Becke, A. D. *Phys. Rev. A* **38**, 3098 (1988).

23. Perdew, J. P. *Phys. Rev. B* **33**, 8822 (1986); Perdew, J. P. *Phys. Rev. B* **34**, 7406 (1986).

24. Eichkorn, K., Weigend, F., Treutler, O. & Ahlrichs, R. *Theor. Chim. Acta* **97**, 119 (1997).

25. Schäfer, A., Huber, C. & Ahlrichs, R. *J. Chem. Phys.* **100**, 5829 (1994).

26. Klamt, A., Eckert, F., Hornig, M., Beck, M. E. & Burger, T. *J. Comp. Chem.* **23**, 275 (2001).

27. Rogers, R. D., Seddon, K. R. & Volkov, S. (eds). *Green Industrial Applications of Ionic Liquids*. NATO Science Series, Kluwer, Dordrecht (2002).

28. Anderson, J. L., Dixon, J. K. & Brennecke, J. F. *Acc. Chem. Res.* **40**, 1208 (2007).

29. Pophale, R., Deem, M.W. & Cheeseman, M.W. *Phys. Chem. Chem. Phys.***13**, 12407 (2011).

30. Kim, J., Martin, R. L., Rubel, O., Haranczyk, M. & Smit, B. *J. Chem. Theory Comput.* **8**, 1684 (2012).

31. Kim, J. & Smit, B. *J. Chem. Theory Comput.* **8**, 2336 (2012).

32. Myers, A. L. & Prausnitz, J. M. *AICHE* **11**, 121 (1965).

33. Garcia-Perez E. et al. *Adsorption* **13**, 469 (2007).

34. Smit, B. & Maesen, T. *Chem. Rev.***108**, 4125 (2008).

35. Fang, H., Kamakoti, P., Zang, J., Cunday, S., Paur, C., Ravikovitch, P., and Sholl D., *J. Phys. Chem. C*, **116**, 10692 (2012).

36. Soler, J. M., Artacho, E., Gale, J. D., Garcia, A., Junquera, J., Ordejón, P, and Sanchez-Portal, D., *J. Phys. Cond. Matter* **14**, 2745 (2002).

37. Wilems, T.F., Rycroft, C.H., Kazi, M., Meza, J.C., and Haranczyk, M., *Micropor. and Mesopor. Materials* **149**, 134 (2012).

38. Kim, J., Lin, L-C., Swisher, J.A., Haranczyk, M., and Smit. B., *J. Am. Chem. Soc.*, **134**, 18940 (2012).

39. Bagheri, N., and Abedi, J., *Chem. Eng. Res. Des.* **89**, 2038 (2011).

40. Chen, J.,Li, W., Li, X., and Yu, H., *Environ. Sci. Technol.* **46**, 10341 (2012).

Acknowledgements

The work at LLNL was performed under the auspices of the U.S. Department of Energy by Lawrence Livermore National Laboratory under Contract DE-AC52-07NA27344. J.K. was supported in part by the U.S. Department of Energy under contract DE-AC02-05CH11231 through the Carbon Capture Simulation Initiative (CCSI). L.-C.L. was supported by the Deutsche Forschungsgemeinschaft (DFG, priority program SPP 1570). B.S. was supported as part of the Center for Gas Separations Relevant to Clean Energy Technologies, an Energy Frontier Research Center funded by the U.S. Department of Energy, Office of Science, Office of Basic Energy Sciences under Award Number DE-SC0001015. This research used resources of the National Energy Research Scientific Computing Center, which is supported by the Office of Science of the U.S. Department of Energy under Contract No. DE-ACO2-05CH11231.

Author contributions

A. M. coordinated the project, led the effort in liquid/ Ionic Liquid systems, and contributed to a large part of manuscript. J. K. and L. C. performed large-scale simulations on the zeolites and wrote the zeolite section of the paper. J. S. contributed to the introduction. R. A. and B. S. provided insightful comments and useful guidance.

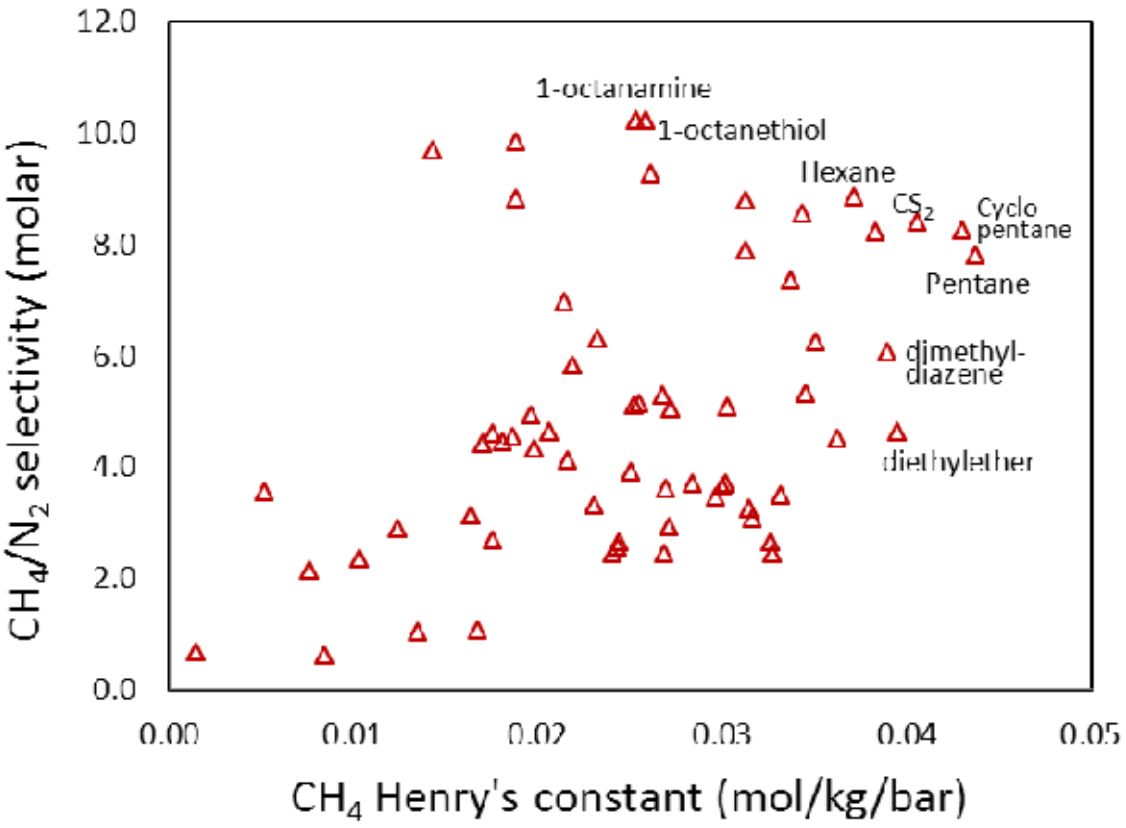

Fig 1. CH_4/N_2 molar selectivity in 73 common liquid solvents plotted against the Henry's constant of methane dissolution. All calculations were performed at T = 25 ^oC and P = 1 bar. The most interesting solvents are indicated.

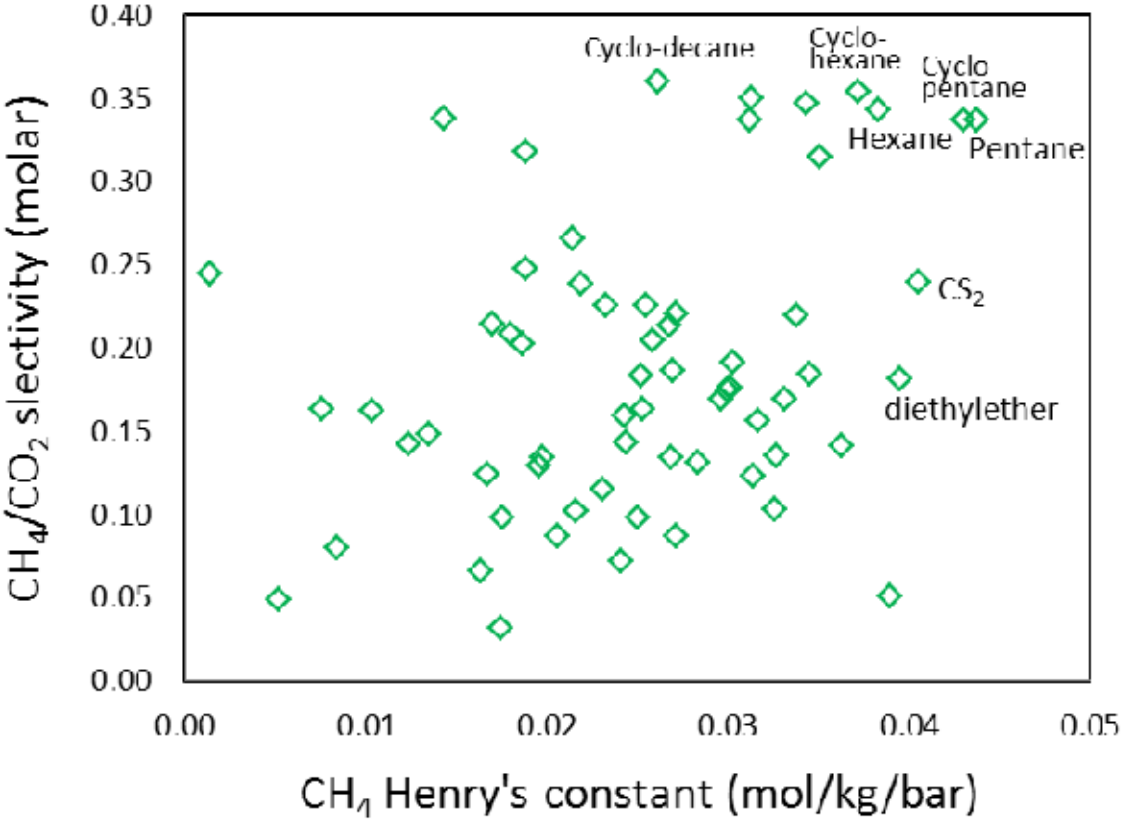

Fig 2. CH_4/CO_2 molar selectivity in the solvents of Fig. 1 plotted against the Henry's constant of methane dissolution. All calculations were performed at T = 25 °C and P = 1 bar. The most interesting solvents are indicated.

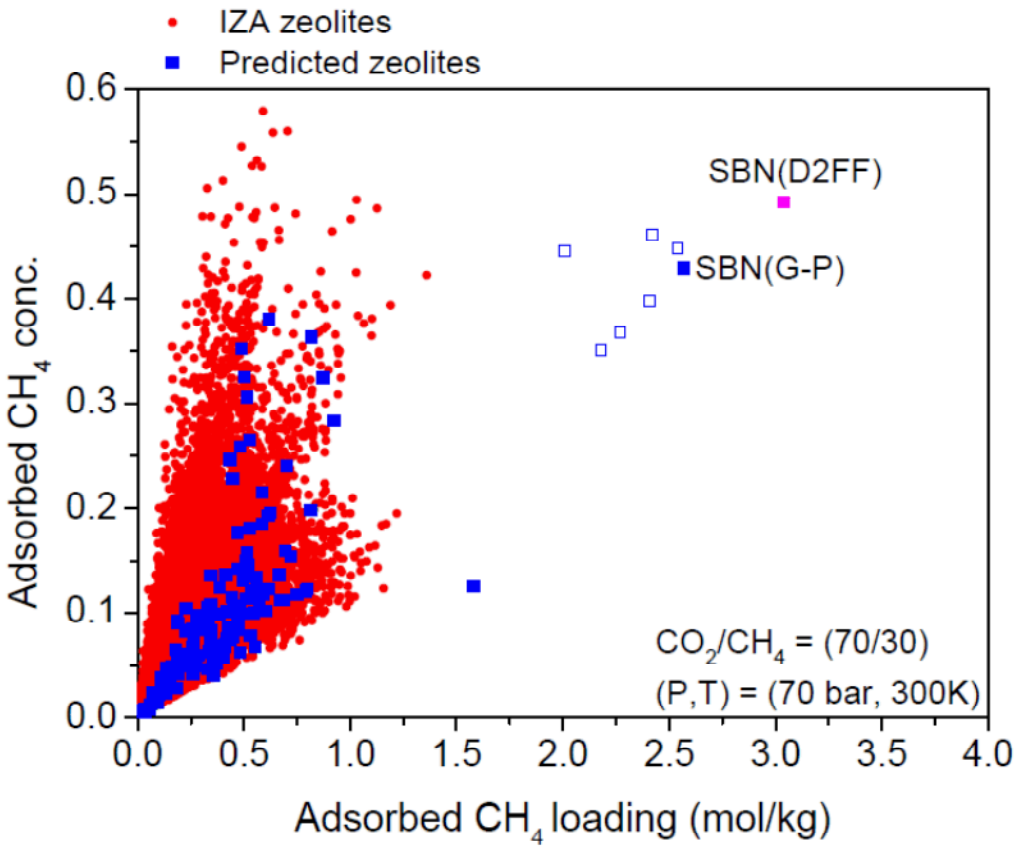

Fig 3. Adsorbed CH_4 concentration as a function of CH_4 loading for 190 IZA (blue) and over 87,000 predicted (red) zeolite structures with initial mixture condition of 30% CO_2 and 70% CH_4 at pressure equal to 70bar and 300K. The SBN, which shows exceptional performance for this separation is plotted for two force fields, Garcia-Perez (blue – solid) and D2FF (pink – solid). The unit cells of the SBN were changed from -3 to 3% of their original sizes, and relaxed using DFT for Garcia-Perez (blue – no fill).

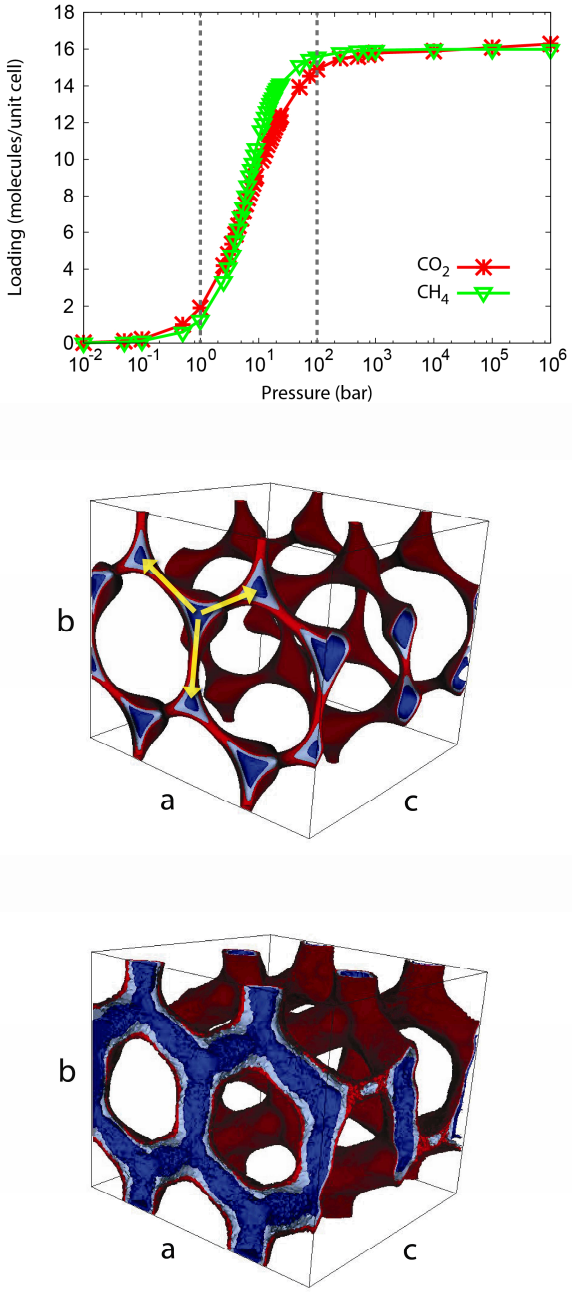

Fig 4. (a) CO_2 (red) and CH_4 (green) adsorption isotherm data at T = 300K where the two curves intersect one another at P=5 bar and P=10^5 bar. The dashed lines divide the isotherms into three important regions: (1) Henry regime, (2) strong CH_4-CH_4 interaction regime, and (3) saturation regime. Free energy landscape inside SBN unit cell for (b) CH_4 and (c) CO_2 molecule with lattice parameters a = 14.374 Angstroms, b = 12.448 Angstroms, and c = 13.846 Angstroms. Dark blue represents low energy strong binding sites with red representing high energies. The three yellow arrows separate one binding site to another and the distance values range from 4-4.6 Angstroms.

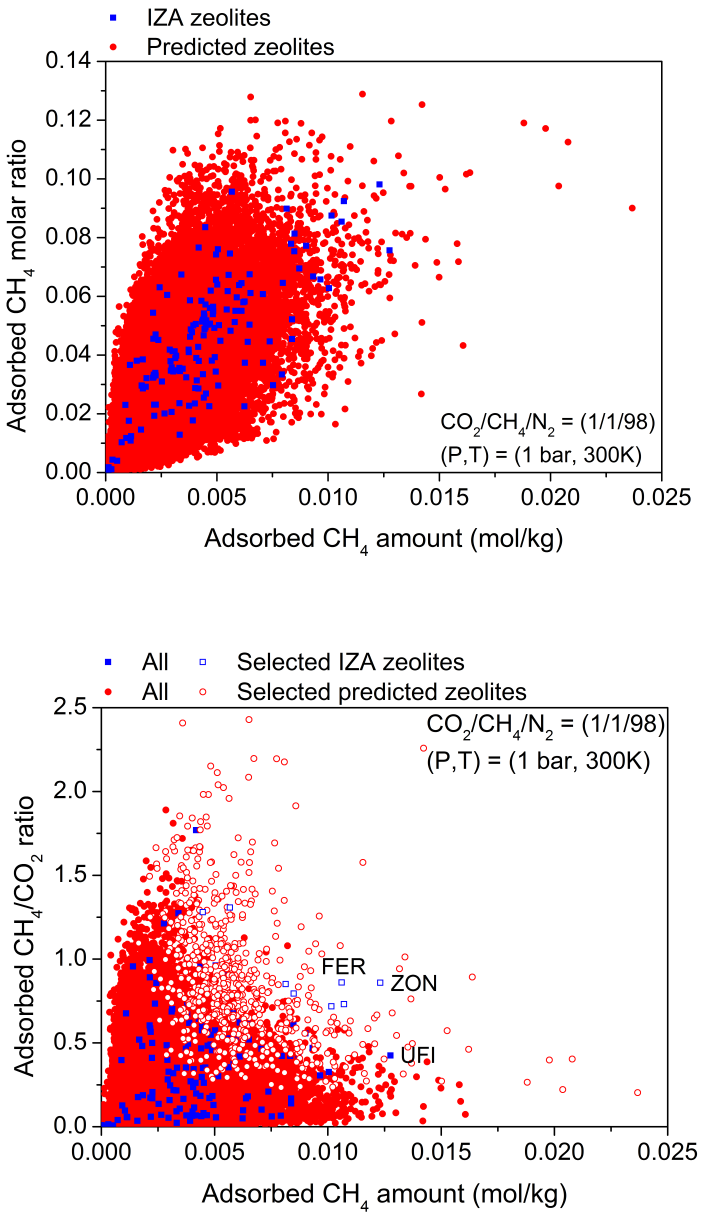

Fig 5.(a) Adsorbed CH_4 concentration as function of CH_4 loading for IZA (blue) and predicted (PCOD) (red) structures. (b) The same data points are plotted with Adsorbed CH_4/CO_2 ratio as a function of adsorbed CH_4 amount. The "no fill" data points represent zeolite structures from Fig. 5(a) that have adsorbed CH_4 molar ratio > 0.08. Thus the best structures are structures within the set of "no fill" data points that also have large adsorbed CH_4 amount and large CH_4/CO_2 ratio values.